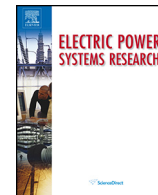




Contents lists available at ScienceDirect

# Electric Power Systems Research

journal homepage: [www.elsevier.com/locate/epsr](http://www.elsevier.com/locate/epsr)



## Transients caused by switching of 420 kV three-phase variable shunt reactor

Alan Župan <sup>a</sup>, Božidar Filipović-Grčić <sup>b,\*</sup>, Dalibor Filipović-Grčić <sup>c</sup>

<sup>a</sup> Croatian Transmission System Operator Ltd., Kupska 4, Zagreb 10000, Croatia

<sup>b</sup> Faculty of Electrical Engineering and Computing, University of Zagreb, Zagreb 10000, Croatia

<sup>c</sup> Končar Electrical Engineering Institute, Zagreb 10000, Croatia

### ARTICLE INFO

#### Article history:

Available online xxx

#### Keywords:

Variable shunt reactor  
SF<sub>6</sub> circuit breaker  
Controlled switching  
Inrush current  
Electric arc model  
EMTP-RV simulations

### ABSTRACT

This paper describes transients caused by uncontrolled and controlled switching of three-phase 420 kV variable shunt reactor (VSR). The model for the analysis of the transients caused by switching of VSR was developed in the EMTP-RV software. It includes a dynamic electric arc in SF<sub>6</sub> circuit breaker and the model of substation equipment. Inrush currents due to VSR energization and overvoltages due to de-energization were determined at tap positions corresponding to lowest 80 MVA and highest 150 MVA reactive power. Based on the calculation results, mitigation measures and operating switching strategy of VSR were proposed.

© 2015 Elsevier B.V. All rights reserved.

## 1. Introduction

The function of shunt reactors in transmission networks is to consume the excessive reactive power generated by overhead lines under low-load conditions, and thereby stabilize the system voltage. They are quite often switched on and off on a daily basis, following the load situation in the system. Instead of having two or more shunt reactors with fixed power ratings, a single variable shunt reactor (VSR) could be used for compensation of reactive power.

The actual magnitude of the inrush current due to VSR energization is quite dependent on the range of linearity of the VSR core and on the time instant of circuit breaker pole operation. Switching operations at unfavorable instants can cause inrush currents that may reach high magnitudes and have long time constants. In case when VSRs have a solidly grounded neutral, unsymmetrical currents cause zero-sequence current flow, which can activate zero-sequence current relays. This may cause difficulties such as unwanted operation of the overcurrent relay protection [1].

De-energization of the VSR can impose a severe duty on both the shunt reactor and its circuit breaker due to current chopping that occurs when interrupting small inductive currents. The switching overvoltages can be dangerous for the equipment if the peak value exceeds the rated switching impulse withstand voltage of the

VSR. However, the overvoltages resulting from the de-energization are unlikely to cause an insulation breakdown of VSRs as they are protected by surge arresters connected to their terminals. The severity of the switching duty increases when single or multiple reignitions occur. Such voltage breakdowns create steep transient overvoltages on VSR with the front time ranging from less than one microsecond to several microseconds and may be unevenly distributed across the VSR winding. So these steep fronted transient voltages are stressing the entrance turns in particular with high inter-turn overvoltages. Therefore some mitigation measures should be considered to reduce the chopping overvoltages and the risk of reignition of the circuit breakers.

Uncontrolled switching of shunt reactors, shunt capacitors and transmission lines may cause severe transients such as high overvoltages or high inrush currents [2]. Conventional countermeasures such as pre-insertion resistors, damping reactors or surge arresters can be used to limit the switching transients. In addition, system and equipment insulation can be upgraded to withstand the dielectric stresses. These methods, however, may be inefficient, unreliable or expensive, and do not treat the root of the problem [3].

Controlled switching is a method for eliminating harmful transients via time controlled switching operations. Closing or opening commands to the circuit breaker are delayed in such a way that switching occurs at the optimum time instant related to the voltage phase angle. Controlled switching has become an economical substitute for a closing resistor and is commonly used to reduce switching surges. The number of installations using controlled switching has increased rapidly due to satisfactory

\* Corresponding author. Tel.: +385 1 6129 714; fax: +385 1 6129 890.

E-mail addresses: [alan.zupan@hops.hr](mailto:alan.zupan@hops.hr) (A. Župan), [\(B. Filipović-Grčić\)](mailto:bozidar.filipovic-grcic@fer.hr), [\(D. Filipović-Grčić\)](mailto:dfilipovic@koncar-institut.hr).

**Table 1**  
VSR data.

Rated voltage	420 kV
Rated frequency	50 Hz
Reactive power	150 MVar (tap position 1) 80 MVar (tap position 29)
Rated current	206 A
Core type	Five limb
Total losses (at 420 kV)	232 kW
Zero sequence impedance	1.2 kΩ per phase 2.2 kΩ per phase
Capacitance of winding to ground	3.8 nF per phase

service performance since the late 1990s [4,5]. Currently, it is often recommended for shunt capacitor and shunt reactor banks because it can provide several economic benefits such as the elimination of closing resistors and the extension of a circuit breaker nozzle and contact maintenance interval. It also provides various technical benefits such as improved power quality and the suppression of transients in transmission and distribution systems [6].

This paper describes the transients caused by the switching of a three-phase 420 kV VSR. The inrush currents due to VSR energization and the overvoltages due to de-energization were analyzed. For this purpose, a model of VSR, substation equipment and electric arc in SF<sub>6</sub> circuit breaker was developed in the EMTP-RV software.

## 2. Model in EMTP-RV

The VSR considered in this paper has 29 tap positions, and the tap-changing order is in opposite direction, i.e. it starts from tap position 29 (lowest amount of 80 MVar consumption) and the final position is 1 (highest amount of 150 MVar consumption). The VSR lowers the voltage by tapping from tap position 29 to tap position 1. VSR manufacturer data are shown in Table 1.

Fig. 1 shows the change of VSR reactive power, current and impedance with respect to tap position.

VSR switching transients were calculated only in case of lowest (80 MVar) and highest (150 MVar) reactive power. The calculation of inrush currents requires an adequate modeling of the reactor nonlinear flux-current curve. The nonlinearity is caused by the magnetizing characteristics of the VSR iron core. Recorded RMS voltage-current curves obtained from manufacturer were converted into instantaneous flux-current saturation curves (Fig. 2) which were used in the nonlinear inductance model in EMTP-RV [7] and approximated with two segments (linear area A-B, below knee of the saturation curve and saturation area B-C).

Each phase of a three phase VSR was modeled as a nonlinear inductance with a serially connected resistance  $R_{Cu} = 1.36 \Omega$ ,

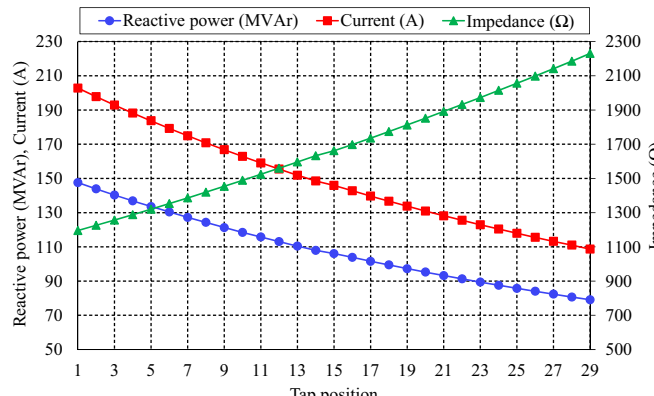


Fig. 1. VSR power, current and impedance versus tap position.

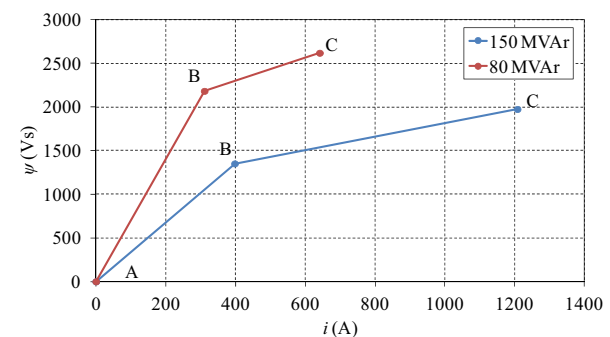


Fig. 2. Instantaneous flux-current saturation curve of VSR.

representing the copper losses, and a parallel connected  $R_{Fe} = 3.04 \Omega$ , representing the iron losses. The magnetic coupling between the three star connected phases was represented with a zero-sequence inductance  $L_0 = 3.7 \text{ H}$  which provides a path for the zero sequence current [8].

The VSR model in EMTP-RV is shown in Fig. 3

The equivalent 420 kV network was represented with positive ( $R_1 = 1.1 \Omega$ ,  $L_1 = 47.13 \text{ mH}$ ) and zero ( $R_0 = 3.14 \Omega$ ,  $L_0 = 64.87 \text{ mH}$ ) sequence impedances, determined from single-phase and three-phase short circuit currents.

The equipment in the high voltage substation was represented by surge capacitances [9], whereas busbars and connecting leads by a frequency dependent line model. MO surge arresters in the VSR bay of rated voltage  $U_r = 330 \text{ kV}$  were modeled with a nonlinear  $U-I$  characteristic with respect to switching overvoltages.

SF<sub>6</sub> circuit breaker with two breaking chambers was represented by the Schwarz-Avdonin electric arc model [10,11] and grading capacitors of 500 pF connected in parallel to the breaking chambers. The EMTP-RV model shown in Fig. 4 consists of the equivalent 420 kV network, the main busbars, the SF<sub>6</sub> circuit breaker and equipment in VSR bay.

## 3. Uncontrolled energization of VSR

The following instants of circuit breaker pole closing were considered:  $t_A = 15 \text{ ms}$ ,  $t_B = 13 \text{ ms}$  and  $t_C = 17 \text{ ms}$  (Fig. 5). Simulations were carried out in case of the VSR lowest (80 MVA) and highest (150 MVA) reactive power.

### 3.1. Tap position 1: Reactive power 150 MVA

Figs. 5 and 6 show calculated VSR voltages and currents, respectively. The highest inrush current occurs at an instant near the voltage zero-crossing in phase A, since it results with the maximum DC component of current.

The conducted simulation showed that a transient inrush current with an amplitude of 4.27 p.u. and a high DC component lasted for 3.2 s (Fig. 7). This could cause difficulties such as unwanted operation of the overcurrent relay protection.

A zero-sequence current occurred in case of uncontrolled reactor energization (Fig. 8) as a consequence of asymmetry. This may cause a false operation of the relay protection used for detecting single phase-to-ground faults.

### 3.2. Tap position 29: Reactive power 80 MVA

Figs. 9–12 show calculation results. The conducted simulation showed that a transient inrush current with an amplitude of 2.16 p.u. and a high DC component lasted for 4 s (Fig. 11). The inrush and zero-sequence currents were significantly lower in this case compared to the case corresponding to 150 MVA (Fig. 12).

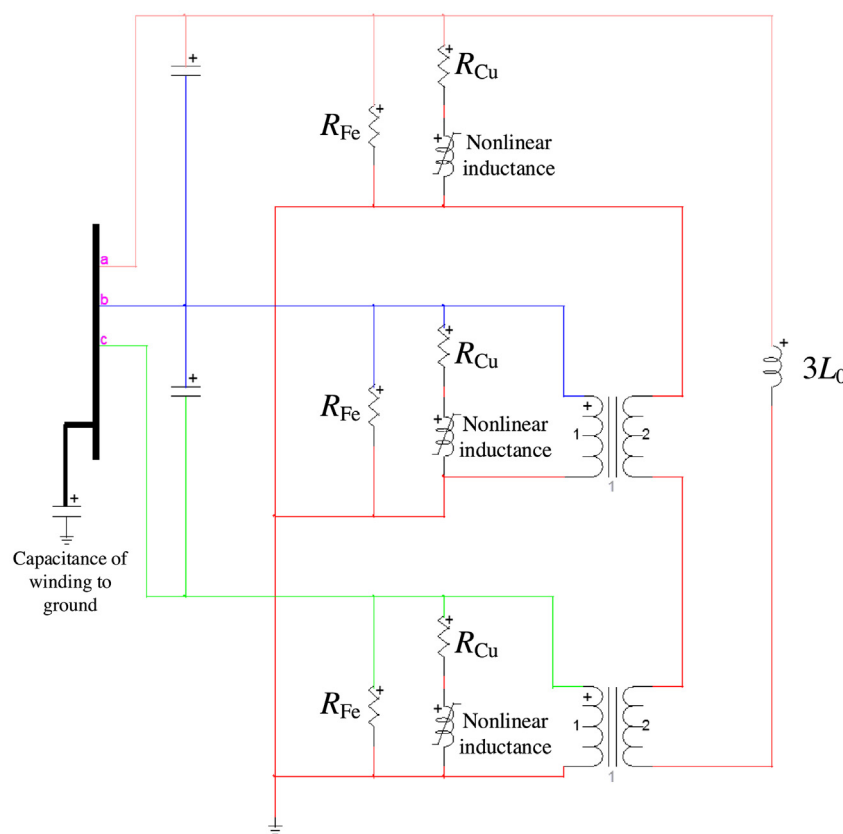


**Fig. 3.** VSR model in EMTP-RV.

#### 4. Controlled energization of VSR

Controlled energization at optimum instants of circuit breaker poles closing at peak voltage 342.93 kV in all phases was analyzed (Fig. 13).

##### 4.1. Tap position 1: Reactive power 150 MVA

Figs. 13 and 14 show VSR voltages and currents.

The current in phase A (Fig. 14) was slightly higher than in the other two phases, due to the appearance of the DC component,

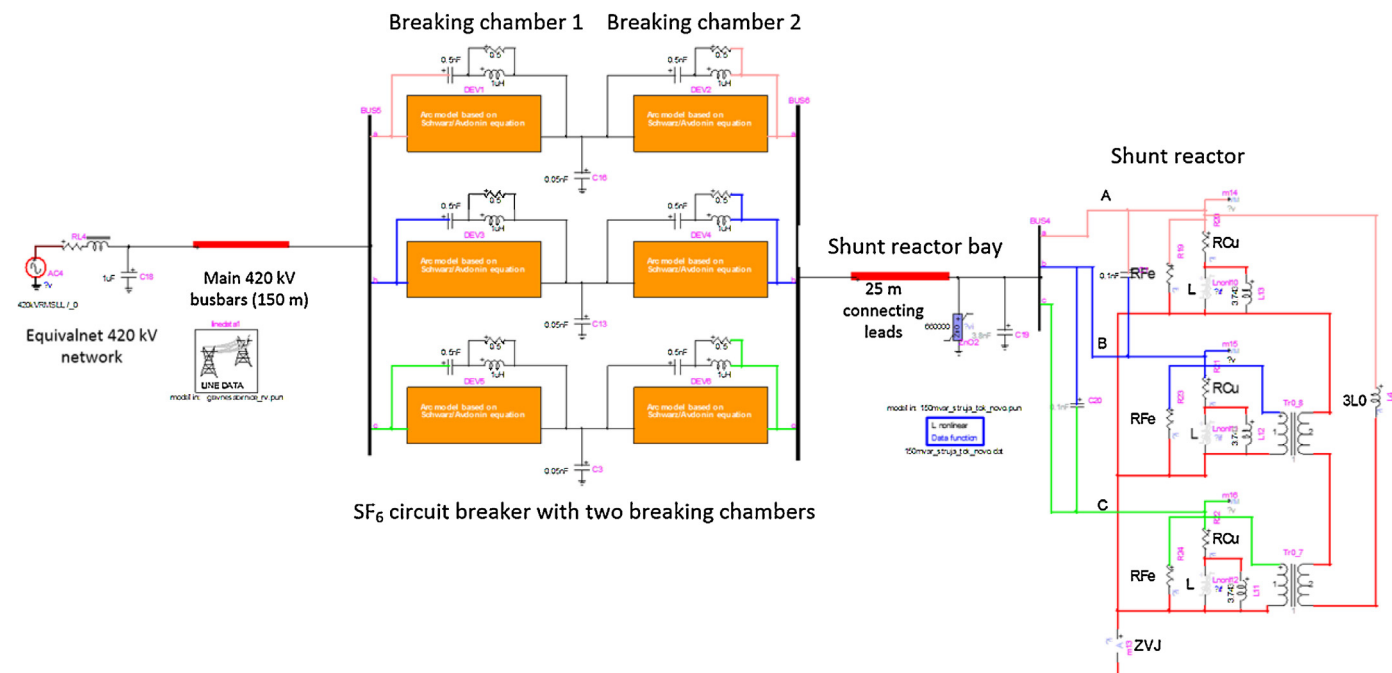


**Fig. 4.** EMTP-RV model of VSR, equipment in substation and equivalent network.

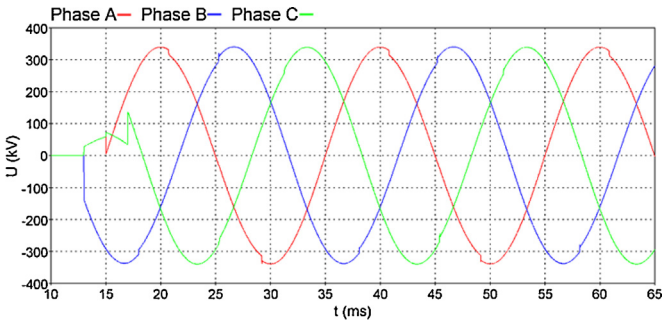


Fig. 5. VSR voltages.

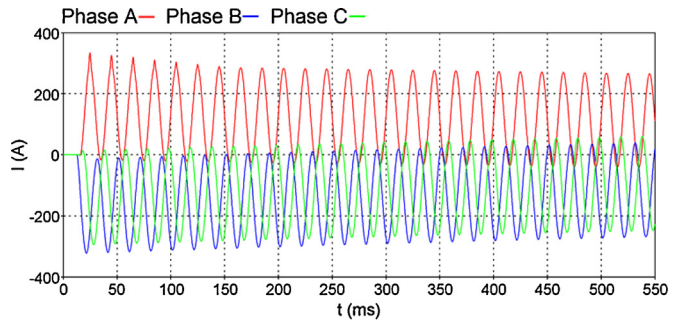
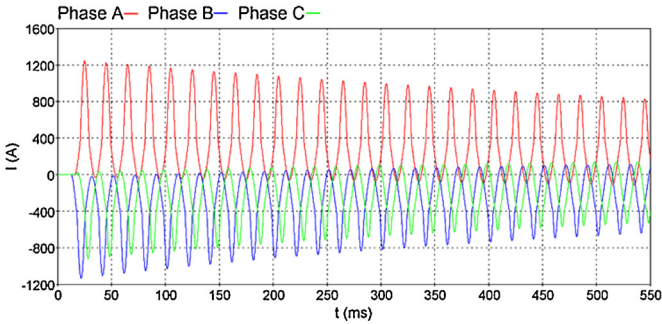
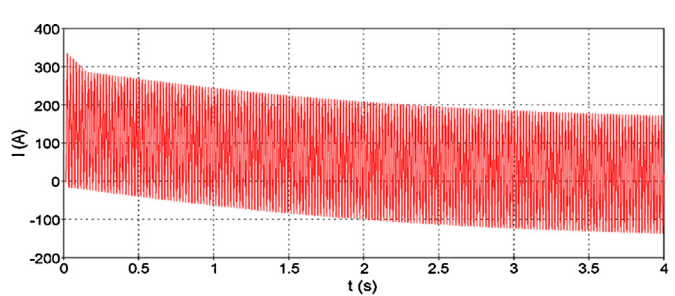
Fig. 10. VSR currents:  $I_{A\max} = 334.2$  A (2.16 p.u.).Fig. 6. VSR currents:  $I_{A\max} = 1245.2$  A (4.27 p.u.).

Fig. 11. VSR current in phase A.

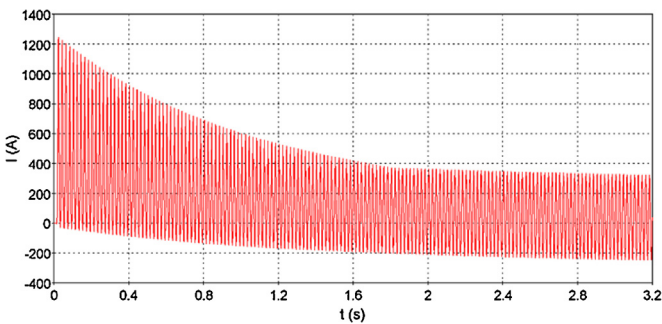


Fig. 7. VSR current in phase A.

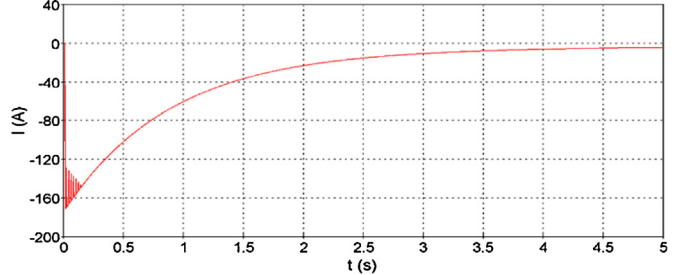
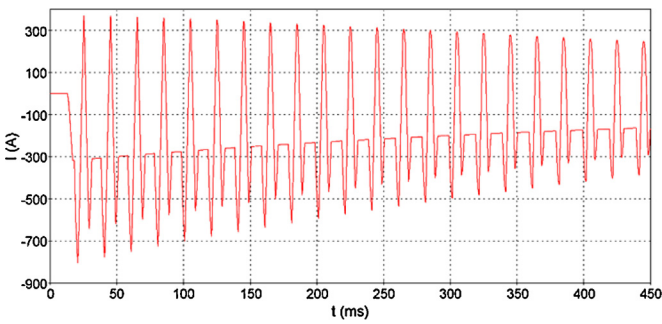
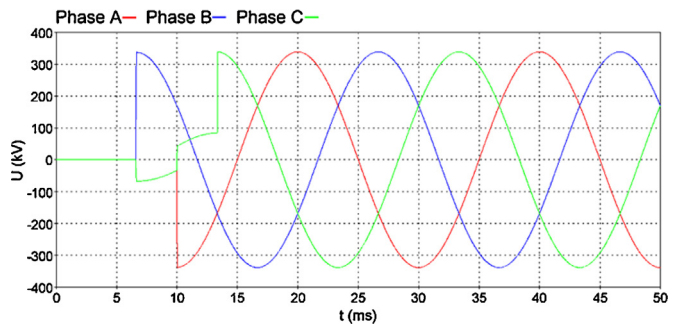
Fig. 12. VSR zero-sequence current,  $I_{\max} = -171.5$  A (1.11 p.u.).Fig. 8. VSR zero-sequence current,  $I_{\max} = -806$  A (2.76 p.u.).

Fig. 13. VSR voltages.

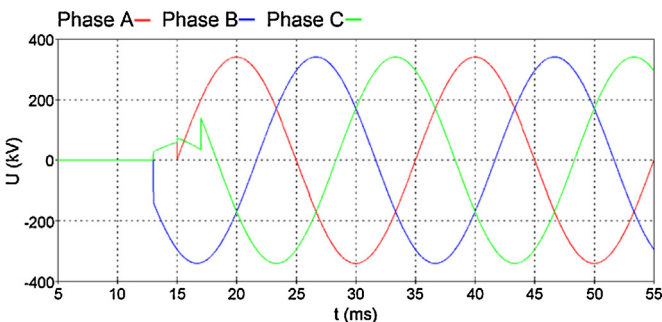
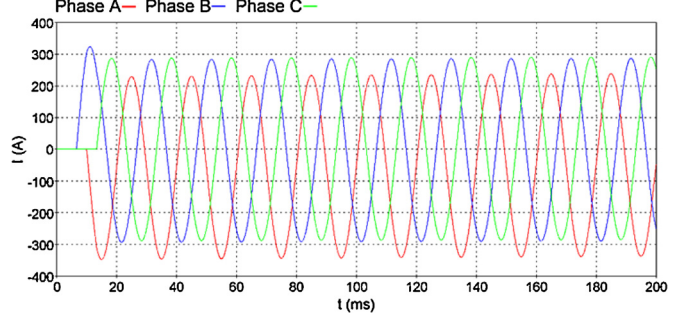


Fig. 9. VSR voltages.

Fig. 14. VSR currents,  $I_{A\max} = -347.8$  A (1.19 p.u.).

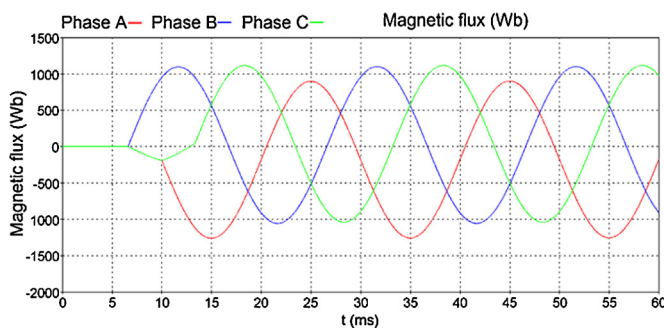


Fig. 15. Magnetic flux in case of VSR controlled energization.

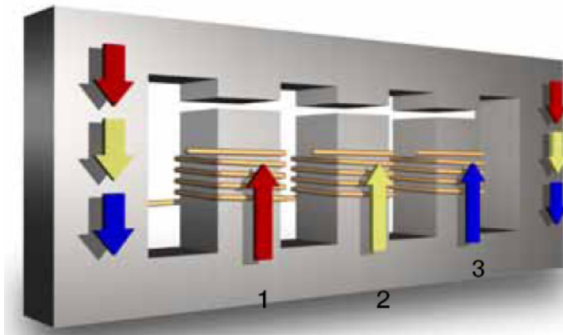


Fig. 16. The distribution of the magnetic flux in the five limb core of VSR—phase A (1), B (2) and C (3).

which was caused by initial magnetic flux in the core limb at the moment of energization. This initial magnetic flux is a part of a magnetic flux from the phase B, which was firstly switched on (Fig. 15). The final distribution of the magnetic flux in the reactor core is shown in Fig. 15.

Due to the air gaps (Fig. 16) utilized in VSR core there were no severe saturation effects [12]. VSR is designed to combine the highest possible inductive power with compact size. For this purpose, iron-cored reactance coils with air gaps are used. The iron core conducts and concentrates the magnetic flux produced by the winding, which has to bridge the air gap. Due to the large difference between the permeability of magnetic sheet steel and oil, it is sufficient to use the magnetic resistance of the air gap for the series connection of the iron and air path. The air gaps reduce inductance and increase the power output of this configuration. The conducted simulation showed that the amplitudes and the DC components of inrush current (Fig. 17) and zero-sequence current (Fig. 18) were significantly lower in case of controlled switching.

As a consequence, a successfully controlled switching reduces the mechanical and electromagnetic stresses of the high voltage

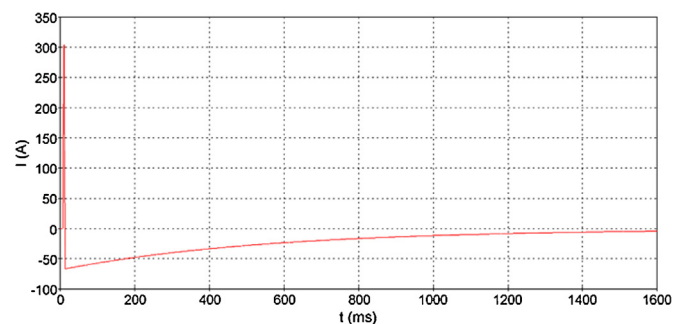


Fig. 18. VSR zero-sequence current.

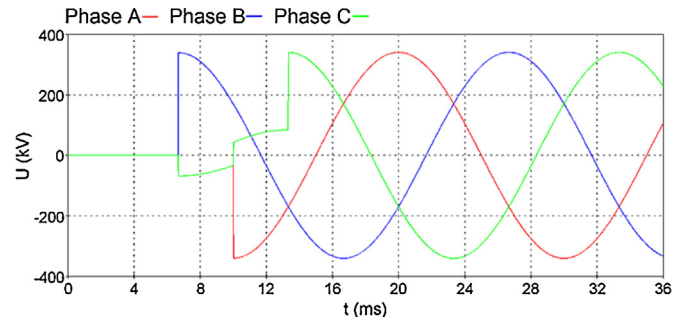
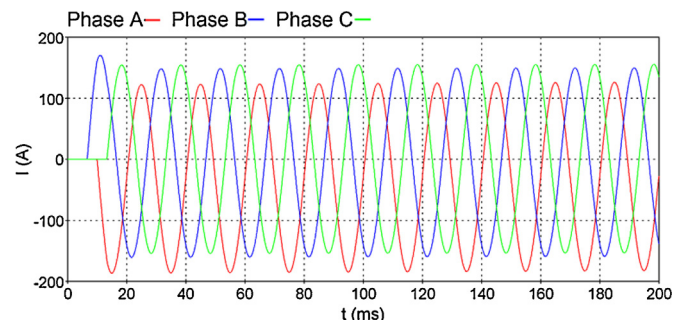


Fig. 19. VSR voltages.

Fig. 20. VSR currents,  $I_{A\text{max}} = -187.0 \text{ A}$  (1.21 p.u.).

equipment and also prevents the unwanted operation of the relay protection.

#### 4.2. Tap position 29: Reactive power 80 MVar

Figs. 19–22 show calculation results in case of 80 MVar. Controlled switching reduced the inrush and the zero-sequence currents, which were lower in case of reactive power 80 MVar compared to 150 MVar.

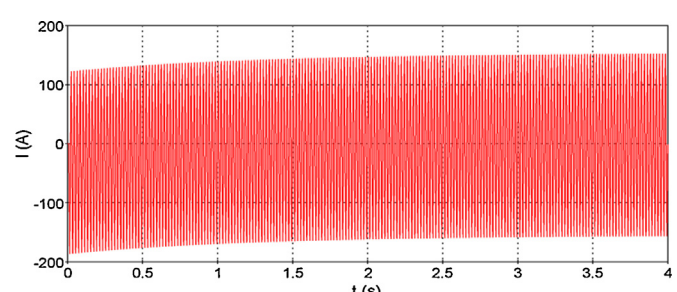


Fig. 21. VSR current in phase A.

**Table 2**

Calculation results in case of 80 MVar.

Phase	Overvoltages on VSR $U_{\max}$ (kV)	TRV on circuit breaker $U_{\max}$ (kV)		
		Breaking chamber 1	Breaking chamber 2	Total TRV
A	469.3	372.5	367.3	667.3
B	446.0	291.7	320.5	612.2
C	477.3	369.1	352.6	721.7

**Table 3**

Calculation results in case of 150 Mvar.

Phase	Overvoltages on VSR $U_{\max}$ (kV)	TRV on circuit breaker $U_{\max}$ (kV)		
		Breaking chamber 1	Breaking chamber 2	Total TRV
A	387.7	322.3	354.3	676.6
B	429.3	302.6	334.1	636.7
C	463.3	393.9	365.0	761.6

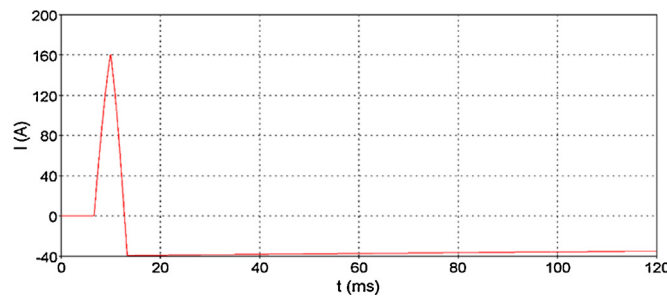
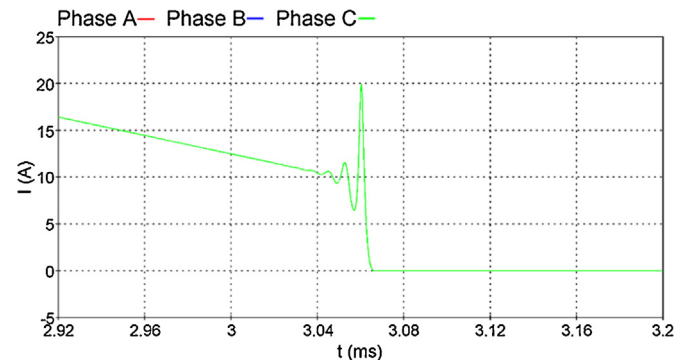
Fig. 22. VSR zero-sequence current,  $I_z\max = 160.4$  A (1.04 p.u.).

Fig. 24. Current chopping in phase C.

## 5. De-energization of VSR

Fig. 23 shows circuit breaker currents in case of 80 MVar de-energization and Fig. 24 shows the current chopping in phase C. For small inductive currents, the cooling capacity of the circuit breaker dimensioned for the short-circuit current is much higher in relation to the energy dissipated in the electric arc. This led to arc instability and the oscillating phenomena shown in Fig. 24 occurred.

During this high frequency oscillation, current crossed through the zero value and the circuit breaker interrupted the current before its natural zero-crossing at the 50 Hz frequency. This phenomenon was followed by a transient overvoltage mainly due to the oscillatory state which was set up on the VSR side. Tables 2 and 3 show the calculated overvoltages on VSR and transient recovery voltages (TRV) on the circuit breaker in the case with surge arresters.

Overvoltages on VSR (Fig. 25) were higher in case of 80 MVar, while TRV on circuit breaker (Fig. 26) was higher in case of

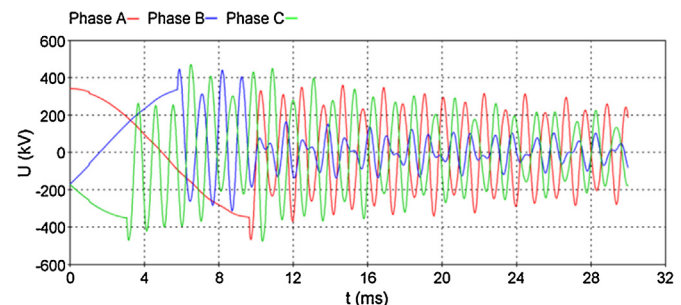


Fig. 25. Overvoltages on VSR (80 MVA).

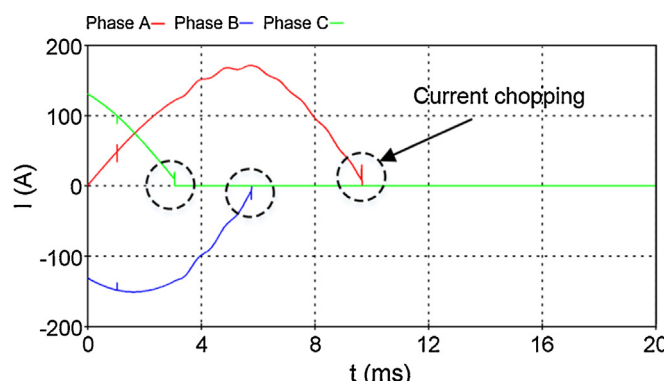


Fig. 23. Circuit breaker currents during the VSR de-energization.

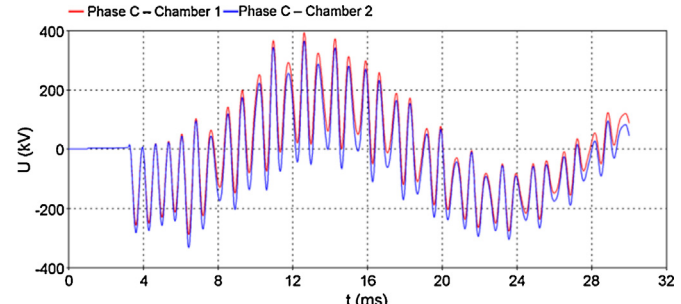


Fig. 26. TRV across breaking chambers in phase C (150 MVA).

**Table 4**

Reduction of TRV and overvoltages on VSR in phase C due to installation of surge arresters.

	150 MVA <sub>r</sub>	80 MVA <sub>r</sub>		
	TRV (kV)	Overvoltages on VSR (kV)	TRV (kV)	Overvoltages on VSR (kV)
Without arresters	791.6	475.6	923.7	659.7
With arresters	761.6	463.3	721.7	477.3

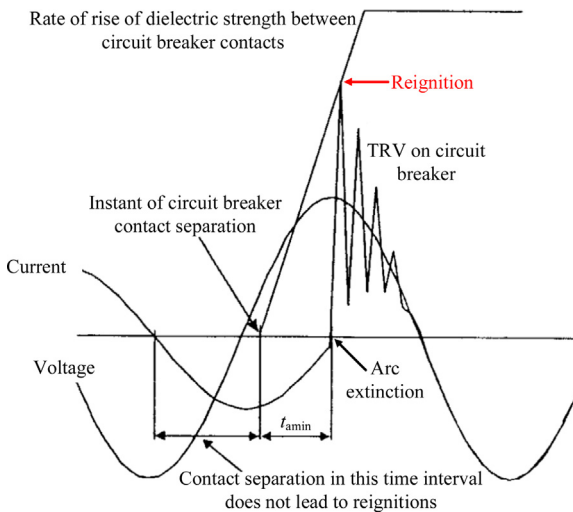


Fig. 27. Target for contact separation in order to eliminate reignitions.

## 6. Overvoltages due to electric arc reignition

Reignition overvoltages are generated by the reignition following the initial interruption and arc extinction. Reignitions are provoked when the TRV across the circuit breaker contacts exceeds the dielectric strength (Fig. 27).

For arcing times shorter than  $t_{\text{amin}}$ , which represents the arcing time at which reignition is still probable, a high probability of reignition exists. Fig. 27 depicts two time instants of contact separation, with and without reignition. Uncontrolled de-energization will, in a typical case, cause reignition in at least one circuit breaker pole. By controlling the contact separation in such a manner that arcing times shorter than  $t_{\text{amin}}$  will not occur, reignitions will be eliminated. The occurrence of reignition depends on system configuration and circuit breaker performances. Reignition can be usually expected near the peak value of the TRV where the voltage difference across the circuit breaker is around 2 p.u. Reignition in phase A at peak value of TRV is shown in Fig. 28 and overvoltages on VSR for 80 MVA<sub>r</sub> in case without surge arresters are shown in Fig. 29.

In this case, steepness of overvoltage in phase A was 376 kV/ $\mu$ s. Table 5 shows calculated overvoltages on VSR due to reignition

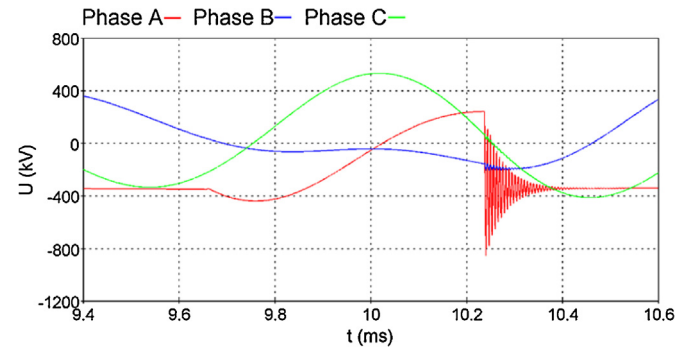


Fig. 29. Overvoltages on VSR due to reignition in phase A at peak value of the TRV.

**Table 5**

Overvoltages due to arc reignition.

	Overvoltages on VSR $U_{\text{max}}$ (kV)	
	150 MVA <sub>r</sub>	80 MVA <sub>r</sub>
Without surge arresters	904.5	857.3
With surge arresters	677.8	673.1

at peak value of TRV in phase A. Overvoltages caused by reignition were not critical considering insulation breakdown of VSR, as it was protected by surge arresters. However, steep wave front overvoltages stress the insulation of the first few winding turns.

## 7. Conclusion

This paper describes switching transients caused by uncontrolled and controlled switching of three-phase 420 kV variable shunt reactor (VSR) at tap positions corresponding to lowest (80 MVA<sub>r</sub>) and highest (150 MVA<sub>r</sub>) reactive power. EMTP-RV model was developed, which includes dynamic behavior of electric arc in SF<sub>6</sub> circuit breaker.

The simulations showed that inrush currents and zero-sequence currents were significantly lower in case of 80 MVA<sub>r</sub> compared to 150 MVA<sub>r</sub>. Therefore, the energization of VSR at 80 MVA<sub>r</sub> is recommended. Controlled energization successfully reduced the amplitudes and DC components of inrush currents and zero-sequence current.

Overvoltages on VSR and transient recovery voltage on circuit breaker were calculated during VSR de-energization. The analysis showed that overvoltages were higher in case of 80 MVA<sub>r</sub>. Therefore, de-energization of VSR at 150 MVA<sub>r</sub> is recommended. MO surge arresters effectively limited both TRV on circuit breaker and overvoltages on VSR, which were lower than switching impulse withstand voltage (1050 kV, 250/2500  $\mu$ s).

Occurrence of reignition near the peak value of TRV was analyzed and reignition overvoltages were lower than lightning impulse withstand voltage (1425 kV, 1.2/50  $\mu$ s) of VSR. However, frequent exposure of VSR insulation to transients, especially steep reignition overvoltages, deteriorates its dielectric properties. In this particular case, calculated overvoltage steepness was lower than 772 kV/ $\mu$ s, recommended by [13].

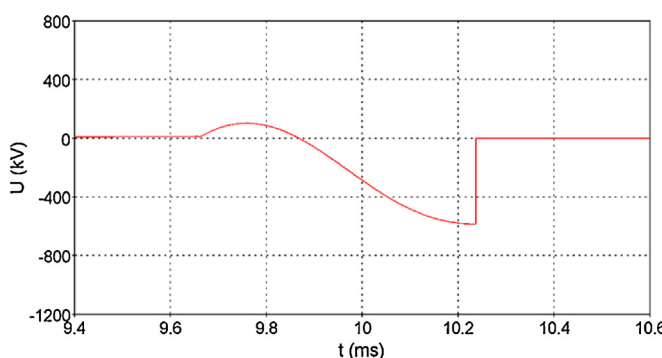


Fig. 28. TRV across circuit breaker in phase A.

The application of VSR controlled switching can completely eliminate the probability of circuit breaker reignition during de-energization.

## Acknowledgement

This work has been supported in part by the Croatian Science Foundation under the project “Development of advanced high voltage systems by application of new information and communication technologies” (DAHVAT).

## References

- [1] Z. Gajić, B. Hillstrom, F. Mekić, HV shunt reactor secrets for protection engineers, in: 30th Western Protective Relaying Conference, Washington, 2003.
- [2] I. Uglešić, B. Filipović-Grčić, S. Bojić, Transients caused by uncontrolled and controlled switching of circuit breakers, in: The International Symposium on High-Voltage Technique Höfler's Days, 7–8 November 2013, Portorož, Slovenia, 2013.
- [3] I. Uglešić, S. Hutter, B. Filipović-Grčić, M. Krepela, F. Jakl, Transients due to switching of 400 kV shunt reactor, in: International Conference on Power System Transients (IPST), June 24–28, 2001, Rio de Janeiro, Brazil, 2001.
- [4] Karcius M.C. Dantas, Washington L.A. Neves, Fernandes Damásio Jr., Gustavo A. Cardoso, Luiz C. Fonseca, On applying controlled switching to transmission lines: case studies, in: International Conference on Power Systems Transients (IPST), June 3–6, 2009, Kyoto, Japan, 2009.
- [5] CIGRE, CIGRE TF13.00.1: Controlled Switching, State-of-the-Art Survey, Part 1: ELECTRA, No.162, pp. 65–96, Part 2: Electra No.164, CIGRE, 1995, pp. 65–96.
- [6] Mitsubishi, Mitsubishi Electric Advance Controlled Switching System, vol. 117, Mitsubishi, Japan, 2007, ISSN 1345-3041.
- [7] J. Mahseredjian, C. Dewhurst, Using EMTP Tutorials and Reference, Hydro-Québec/IREQ, Montreal, Canada, 2008.
- [8] J. Vernieri, B. Barbieri, P. Arnera, Influence of the representation of the distribution transformer core configuration on voltages during unbalanced operations, in: International Conference on Power System Transients (IPST), Rio de Janeiro, 2001.
- [9] F. Ali, D.W. Imece, H. Durbak, S. Elahi, A. Kolluri, D. Lux, T.E. Mader, A. McDermott, A.M. Morched, R. Mousa, L. Natarajan, E. Rugeles, Tarasiewicz, Modeling guidelines for fast front transients, IEEE Trans. Power Delivery 11 (1) (1996) 493–506, Report prepared by the Fast Front Transients Task Force of the IEEE Modeling and Analysis of System Transients Working Group.
- [10] CIGRE, CIGRE Technical Brochure 135: State of the Art of Circuit-breaker Modeling, WG 13.01, 1998.
- [11] B. Filipović-Grčić, D. Filipović-Grčić, I. Uglešić, Analysis of transient recovery voltage in 400 kV SF<sub>6</sub> circuit breaker due to transmission line faults, Int. Rev. Electr. Eng. 6 (5 Part B) (2011) 2652–2658.
- [12] ABB, Controlled Switching, Buyer's & Application Guide, Edition 4, ABB, Ludvika, Sweden, 2013.
- [13] S.A. Morais, Considerations on the Specification of Circuit-Breakers Intended to Interrupt Small Inductive Currents, Electra, No. 147, April 1993, pp. 45–69.